



## Comparative micro-computed tomographic analysis of the structure of brood cells and its effect on the development of the pupae of honey bee (*Apis mellifera*)

TAMÁS SIPOS<sup>1,3</sup>, TAMÁS DONKÓ<sup>1,2</sup>, ÁDÁM CSÓKA<sup>2,3</sup>, TAMÁS KISS<sup>4</sup> and SÁNDOR KESZTHELYI<sup>1</sup>

<sup>1</sup> Hungarian University of Agriculture and Life Sciences, Institute of Agronomy, Kaposvár Campus, Sándor Guba str. 40, H-7400 Kaposvár, Hungary; e-mails: sipostomi97@gmail.com, ostrinia@gmail.com

<sup>2</sup> Medicopus Ltd., Sándor Guba str. 40, H-7400 Kaposvár, Hungary; e-mails: Donko.Tamas@sic.medicopus.hu, Adam.Csoka@sic.medicopus.hu

<sup>3</sup> Hungarian University of Agriculture and Life Sciences, Doctoral School in Animal Science, Kaposvár Campus, Sándor Guba str. 40, H-7400 Kaposvár, Hungary

<sup>4</sup> János Szentágothai Research Centre & Centre for Neuroscience, University of Pécs, Ifjúság str. 20, H-7624 Pécs, Hungary; e-mail: kiss891012@gmail.com

**Key words.** Hymenoptera, Apidae, comb cell volume and size, developmental disorders, computer tomography, wax structure

**Abstract.** Most beekeepers worldwide use the same combs in their hives for many years, which can result in alterations in the inner volume of the comb cells. The objective of this survey using microcomputed tomography was to reveal developmental disorders caused by this beekeeping practice. The extent of the thickening of the wall of brood cells that occurs as a result of the long-term use of the combs was determined. This alteration resulted in a reduction in the inner volume of the comb cells, which had a significant effect on the size of the pupae and possibly the health of the imagoes. The walls of the cells can be divided into two well-determined parts, which can be exactly visualized using micro-CT. In addition, the inner structure of the wall in the first part of the cell was altered by very radio dense remains of cocoons. The material in the other part of the cell is less radio dense and as previously suggested is mainly wax. The decrease in the length, surface and volume of these cells adversely affected the developing pupae, which according to previous studies results in a reduction in the production of workers, colony strength and honey yield. The extent of the reduction in the body regions of pupae was on average 4.98%. Overall, the volume of the pupae that developed in these narrow comb cells were smaller by an average of 12.22%.

### 1. INTRODUCTION

The majority of crops relies on animal pollination and the decline of wild insect pollinators in many agricultural landscapes has made the western honeybee (*Apis mellifera* L. 1758) one of the key elements of global food production and the only source of bee products like wax, royal jelly and bee venom (Winfrey et al., 2011; Garibaldi et al., 2013; Ellis et al., 2020). The 21st century is one of the most difficult times for the beekeeping industry due to several abiotic (drought, heat, temperature fluctuations) and biotic (*Varroa* mites, viruses, *Nosema* spp., *Tropilaelaps* spp., etc.) factors that cause colony losses of 20% every year worldwide (Williams et al., 2010; Dainat et al., 2012; Neov et al., 2019).

Conventional imaging methods, such as light and confocal microscopy, provide detailed images of the internal anatomy of insects, but for this one has to kill or dissect live individuals (Friedrich et al., 2014). Other disadvantages of these techniques are the limitations of repeated scanning of

individuals. X-ray imaging techniques are widely used in the field of entomological research because they are non-invasive (Smith et al., 2016; Alba et al., 2018). While  $\mu$ -CT is mainly used for anatomical studies, due to its resolution being higher than human diagnostic CT, which is used in studies on crop protection for understanding insect biology and analysing the development of damage (Smith et al., 2016; Keszthelyi et al., 2020; Sonenshine et al., 2022). There is, however, only a few references on bee health using computed tomography and 3D imaging (Facchini et al., 2019; Keszthelyi et al., 2021; Sipos et al., 2021).

Most of the studies on bee health are concerned with the pathology of the imago, which provides little information on pathogenesis, especially during the larval and pupal stages. Beekeepers worldwide use their combs for many years, 50% of combs should be replaced annually, but there are cases of the utilization of combs for even up to 6 years (Taha & Al-Kahtani, 2020). This results in several disadvantages, with the reasons for them remaining unknown in

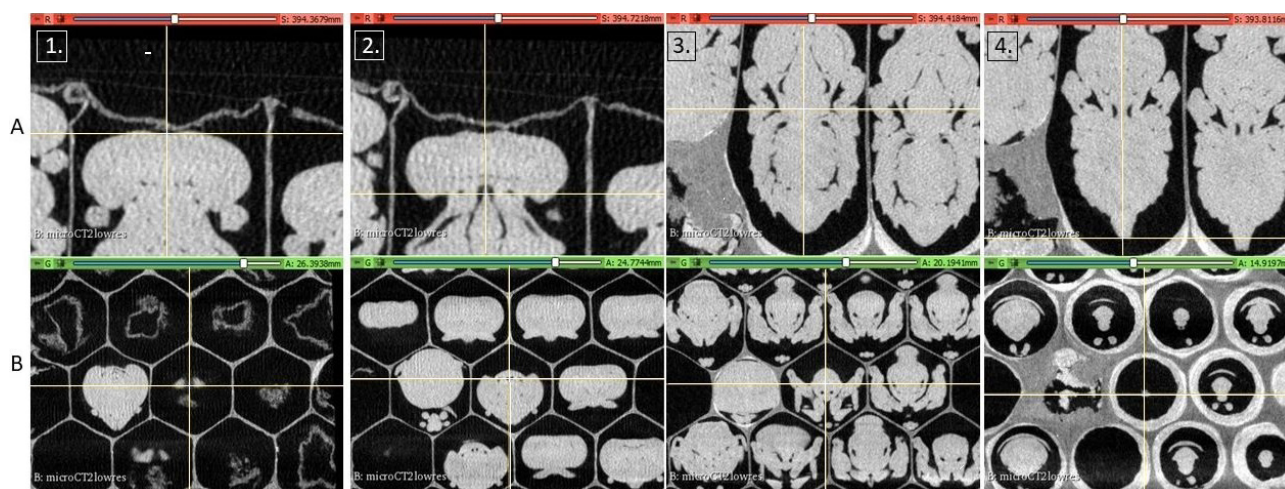


**Fig. 1.** Points used to measure the sizes of body parts of pupae on full layout cross-sectional images.

the majority of cases. Several of the disorders in bee development begin or even occur within the brood cells, which is attributable to improper beekeeping practise. Naturally, the features of these disorders are difficult to determine or are unknown in certain cases. Non-invasive imaging can be used to reveal the developmental processes and anatomical changes that occur due to improper beekeeping practise (Wipfler et al., 2016).

The objective of this study was to determine the reduction in the size of pupae caused by inappropriate beekeeping technology based on the previous results of Berry & Delaplane (2001). First, the extent of the thickening of the brood cell wall that occurs as a result of the use of old combs and its consequences for the size of bee pupae were determined. In addition, the potential significance of modern non-invasive imaging methods, especially computer tomography, in apicultural research is stressed.

## 2. MATERIALS AND METHODS

### 2.1. Origin of comb samples

The brood combs were collected from one *Apis mellifera carnica* colony located on Kaposvár Campus (Somogy county, Hungary; GPS coordinates: WGS: X:46.381079 Y:17.826915) during April. The uniformity of the age of the specimens was provided by the size of the Nagybeczonádi (NB) frame queen confinement cage. The combs contained 18-day-old worker pupae at the pre-imaginal developmental stage. The preparation was done using a scalpel to cut out four pieces of the comb (90 × 60 mm) containing brood from a 3-year-old frame for further selection using medical diagnostic CT. After the human diagnostic measurement, 10 normal and 10 narrow pupae were cut out and used for producing more detailed digital images using  $\mu$ -CT, which was necessary because of the limitations of the  $\mu$ -CT scanning of the length and diameter. The different experimental groups (normal and narrow) were separated visually based on the medical CT imaging. The samples were kept in an incubator under stable environmental conditions at  $34^\circ \pm 0.5^\circ\text{C}$  and  $60\% \pm 10\%$  relative humidity (RH), which are similar to the conditions inside a healthy colony until required for the CT scans.

After the preliminary medical CT visualization, one of the separated comb cells was selected for micro-CT. After this, the remaining pupae were removed and wax of one of the scanned combs was melted. The melting of the wax was done in order

to visualize the different thicknesses of the bottoms of the cells (Fig. 2).

### 2.2. Descriptions of computed tomographic settings and instruments

The  $\mu$ -CT image acquisition was carried out using a Bruker Biospin SkyScan 1176 at the University of Pécs Szentágotthai Research Centre. The samples were examined using the following CT parameters: PANalytical's Microfocus Tube source type, 50 kV source voltage, 500  $\mu\text{A}$  source current, 700 ms exposure time and 0.71 rotation step (deg). NRecon reconstruction program, version 1.7.4.2, was used to produce the final images from raw data. The program created 8bit BMP files with  $3336 \times 3336$  pixels and the pixel size was  $8.74355 \mu\text{m}$ . BMP images were converted to NIFTI (Neuroimaging Informatics Technology Initiative, 2005) files.

The same samples were examined using a Siemens SOMATOM Definition AS+ CT scanner a few hours after the  $\mu$ CT scans using the following parameters: 100 kV tube voltage, 140 mAs X-ray radiation dose, spiral data collection mode with 0.7 pitch, the field of view 50 mm. Standard DICOM (Digital Imaging and Communications in Medicine) images were reconstructed using Siemens Syngo CT VA48A program with convolution kernel V80u. The resolution of the images was  $0.0977 \text{ mm} \times 0.0977 \text{ mm} \times 0.1 \text{ mm}$ . Each series examined was converted from a DICOM to NIFTI (Neuroimaging Informatics Technology Initiative, 2005) file format. The human diagnostic CT was used for preliminary screening and Hounsfield Unit (HU) scaling.

The image post-processing and visualization were done using 3D-Slicer software ([www.slicer.org](http://www.slicer.org)) (accessed on 24 February 2021).

### 2.3. Description of the $\mu$ -CT-based measurements

To determine the density of the different structural parts of a cell, the values produced by  $\mu$ -CT were converted to Hounsfield Units (HU) using the following equation:

$$\text{HU} = \mu\text{-CT voxel value} \times 20.78 - 1024$$

This equation compares the images measured using CT and  $\mu$ -CT. 3D Slicer's Elastix module was used for the rigid registration of the images.

Five, randomly chosen segments represented each of the visually different parts of a cell ( $n = 5$ ). The segment is a manually designated area from the visually distinguished parts of the cell, which contains a slightly different number of voxels due to their manual selection.



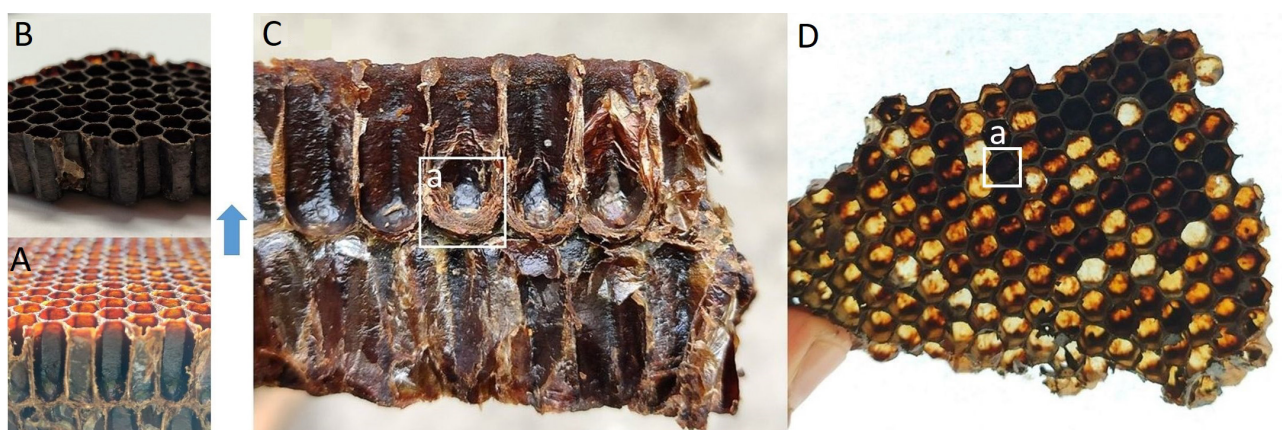


**Fig. 2.** Cells of different sizes in comb. The combs in the frames contain narrow cells (a). A – comb covered with wax; B – fibre-reinforced composite without wax; C – axial cross-section of comb, D – top view of comb.

To establish and compare the volume and surface parameters of different sized brood cells and developing pupae, they were measured using  $\mu$ -CT. This study was based on 10 normal and 10 narrow brood cells determined by preliminary human diagnostic CT screening and then selected visually and marked.

In order to measure developing individuals in 10 normal and 10 narrow cells their lengths (Fig. 1) and volumes were based on  $\mu$ -CT scans. The lengths of their whole body, head, thorax and abdomen were measured using mark-ups. Fiducial mark-ups were placed using 3D Slicer software and Python 3.6 programming language was used for calculating the distances between the marker points. In addition, the relative proportions of the whole body of each body part were measured for specimens from different brood cells.

The surface area and volume of the insects and the inner space of the cells were generated using the segment editor module in the 3D Slicer program. The pupae and the combs were manually segmented utilizing the measured density values of the structural parts of the comb (Fedorov et al., 2012). The information for the segments was generated individually by the segment statistics module.

## 2.5. Statistical analysis

The Kolmogorov-Smirnov test was used to test the morphological data for the pupal stage of honey bees ( $n < 50$ ). For determining whether the data was normally distributed ( $p < 0.05$ ), the Ghasemi- and Zahediasl-type methods were used. The effect of comb cell size on the morphological parameters of this pre-imaginal stage of honey bees was statistically analysed using one-way ANOVA with the help of SPSS 11.5 software. Means were separated using the Tukey (HSD) test, at ( $p \leq 0.05$ ).

## 3. RESULTS

### 3.1. Structural analysis of comb cells of different sizes using $\mu$ -CT

The first picture shows a piece of used comb after brood was removed (Fig. 2A). The structure of the fibre-reinforced material remaining after the removal of wax clearly reveals the remains of the pellicle and cocoon of the previous generations reared in the cells (Fig. 2B). Most visible, however, is that the wall and especially the bottom of some cells are thicker and more enlarged than those of the cells that are even directly adjacent to them. Differences in the wall and bottom thickness of individual cells are seen in

both cross-sections (Fig. 2C) and top-view (Fig. 2D) of light transmitted perspectives.

The  $\mu$ -CT analysis of the comb still containing wax reveals structural differences between normal and narrow cells (Fig. 3). It is clear that the structural components differ in colour in the images, which is due to different radiodensity values. The walls of cells consist of two distinct parts, which can also be visualized using  $\mu$ -CT. The first part surrounding the inner surface is brighter (Fig. 3b). This part is composed of a fibre-reinforced composite product (FRP), which originated from developing pupae, for instance the spinning of a silken cocoon, residues of stored pollen and remains of moulted pellicle. The second part is darker, due to the presence of wax (Fig. 3a), that is composed of a fibre-reinforced composite product with wax (FRPW).

The average volume of normal cells was  $234.103 \pm 4.105 \text{ mm}^3$ . In contrast, that of the narrow cells with thick walls

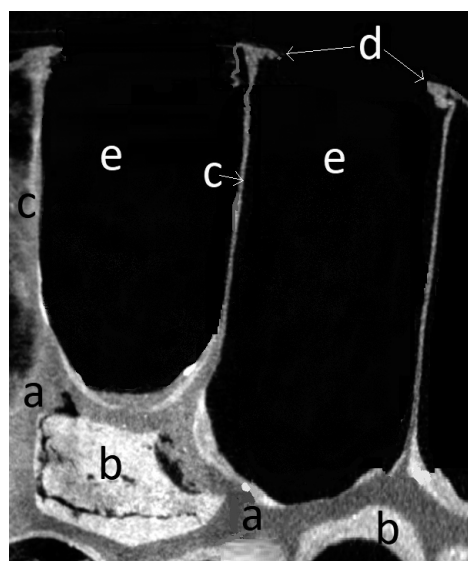


**Fig. 3.** Vertical section of narrow cells obtained using  $\mu$ -CT. a – fibre-reinforced composite with wax (FRPW); b – fibre-reinforced composite without wax (FRP); c – wall of cell, d – remains of capping material of brood cell; e – interior space of cell.

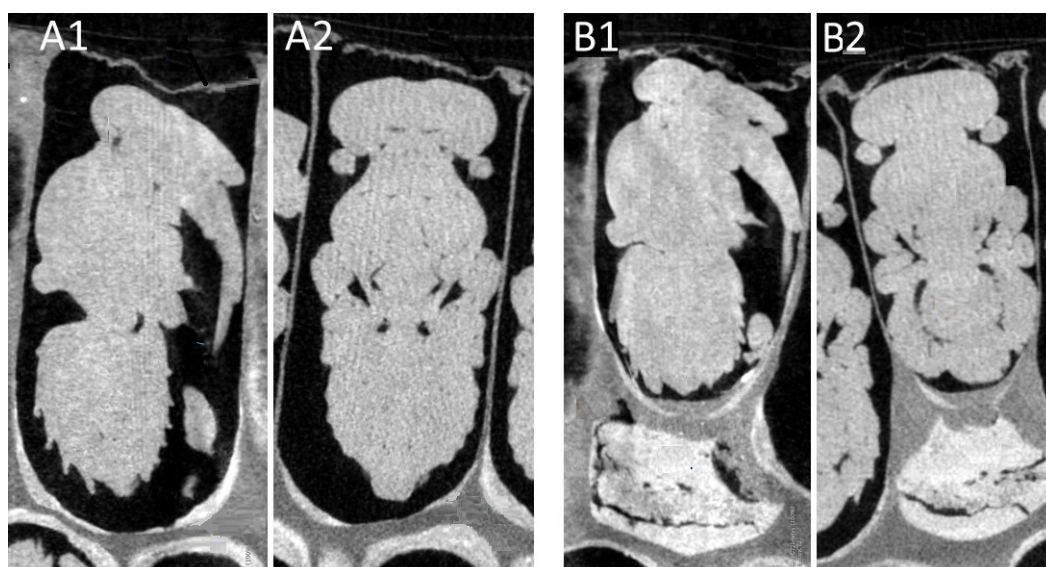


**Fig. 4.** Sections of honey bee pupae in cells obtained using  $\mu$ -CT. A1 – sagittal record of honey bee pupa in a normal cell; A2 – axial record of honey bee pupa in a normal cell; B1 – sagittal record of honey bee pupa in narrow cell; B2 – axial record of honey bee pupa in narrow cell.

were  $151.237 \pm 4.957 \text{ mm}^3$ , which is significantly different ( $p \leq 0.05$ ). The volume of narrow brood cells was 35.41% lower than that of normal comb cells.

The thickened regions in the wall and bottom of cells mainly contain the so-called FRP fraction of the insect developmental origin. Density indices (HU) of the different structural components of the comb also indicate the different positions of each component in the structure of the cells (Table 1). The FRP is mainly included in the formation of the cell wall and build up at the bottom of the cells. This fraction is primarily responsible for the abnormal thickening of the cell, which causes a significant loss of brood cell volume. The primary role of the waxy FRPW fraction is in the capping of the brood cells.

The density of different parts of the comb is statistically different ( $p < 0.05$ ). This is the case for both structurally different (FRP-FRPW) and spatially different components of comb cells. The density of the wax component (FRPW) is lower than that of the brood components attributable to the development of bees (FRP). This is supported by the density of the spatially different cell structures. The cell wall has a slightly denser composition than the higher wax content structures like the capping of the brood cells.

**Table 1.** Radio density values (HU) (mean  $\pm$  SE) of the different parts of comb cells ( $n = 20$ ).

Parts of cell	Radio density (HU) (mean $\pm$ SE)
FRPW (a)	$-422.48 \pm 13.91^a$
FRP (b)	$162.99 \pm 4.03^b$
Wall of comb cell (c)	$-310.13 \pm 10.85^a$
Tapping remains of brood cell (d)	$-342.51 \pm 3.95^b$
The air in the brood cell (e)	$-991.19 \pm 1.77^c$

a, b, c – small letters indicate significant differences ( $p \leq 0.05$ ); FRPW – fibre-reinforced composite with wax; FRP – fibre-reinforced composite.

### 3.2. The effect of different sized comb cells on the development of honey bee pupae

Egg-laying and the development of honey bees occurs naturally in narrow comb cells with a small volume. This results, however, in developmental disorders at the pupal stage of workers (Fig. 4). Individuals developing in these cells are smaller than those developing in normal brood cells. The relative proportions of the body may even change (Table 2). The differences in the size of pupae is well illustrated in the 3 dimensional figure (Fig. 5).

The mean surface area of pupae developing in normal cells was  $266.86 \pm 2.23 \text{ mm}^2$ , whereas that of the pupae developing in narrow cells with thick walls was  $218.97 \pm 1.94 \text{ mm}^2$ . These values are statistically different ( $p \leq 0.05$ ), which indicates that the average surface area of pupae developing in narrow cells, resulting from intensive use, was about 17.94% lower than that of pupae developing in normal brood cells.

The average volume of pupae developing in normal cells was  $120.61 \pm 1.43 \text{ mm}^3$  and of those developing in narrow cells was  $105.87 \pm 1.29 \text{ mm}^3$ . These values are also statistically different.

**Table 2.** Length (mean  $\pm$  SE) of honey bee pupae in normal and narrow cells measured using micro CT on the 18<sup>th</sup> day of postembryonic development ( $n = 10$ ).

		Length (mm)	Ratios	
			Length	dr (%)
Normal	head (a)	$1.41 \pm 0.05^a$	a/b	0.29
	thorax (b)	$4.74 \pm 0.05^b$	d/a	7.84
	abdomen (c)	$5.03 \pm 0.04^c$	d/b	2.33
	whole body (d)	$11.06 \pm 0.05^d$	d/c	2.19
Narrow	head (a)	$1.16 \pm 0.18^e$	a/b	0.32
	thorax (b)	$3.60 \pm 0.09^f$	d/a	7.64
	abdomen (c)	$4.15 \pm 0.07^g$	d/b	2.46
	whole body (d)	$8.87 \pm 0.11^h$	d/c	2.13

dr – degree of reduction; a, b, c, d, e, f, g, h – small letters indicate significant differences ( $p \leq 0.05$ ).



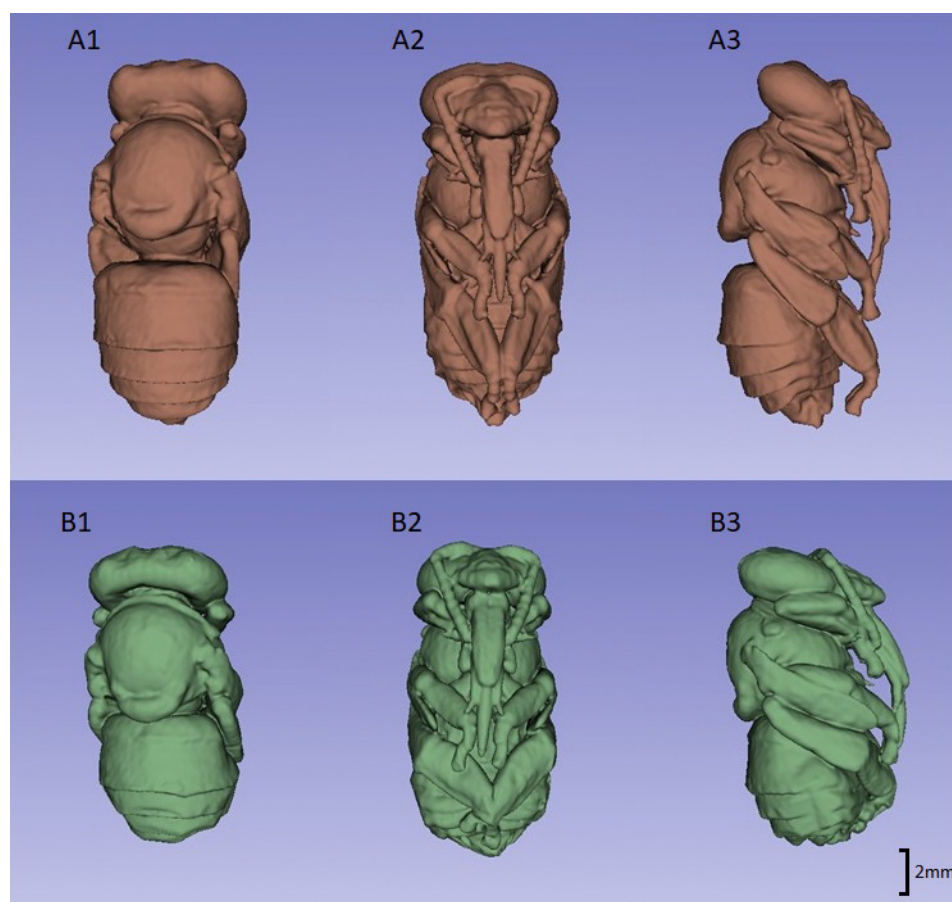


**Fig. 5.** 3D images of honey bee pupae that developed in different sized brood cells. A – pupa from a normal cell; B – pupa from a narrow cell; 1 – dorsal; 2 – ventral; 3 – lateral view.

cally different ( $p \leq 0.05$ ), which indicates, as above, that pupae developing in narrow cells are in terms of volume 12.22% smaller.

Table 2 shows the length of 18-day-old pupae developing in normal and narrow cells. This reveals that in terms of the length of the body and main body parts the development of the bee in narrow cells is distorted. The degree of reduction in the different parts of the body ranges from 2.55 to 9.37%. In relation to the total body length, the greatest reduction was recorded for the thorax size of the developing pupae. This has consequences in terms of reductions in the length of the abdomen and head. The lengths of the pupae originating from the normal and narrow cells differed significantly for each of the body parts measured ( $p \leq 0.05$ ).

#### 4. DISCUSSION

The differences in the bottoms of comb cells was unequivocally confirmed using CT. It was further confirmed that the alterations in the inner volume of the cells resulting from rearing several generations in them had adverse effects on the preimaginal development of honey bees (Berry & Delaplane, 2001). As a result of this ontogenetic effect the cell walls gradually become darker and more brittle, which is also reported by Hepburn (1998). The cells with extremely thick bottoms are in those parts of the comb most intensively used for rearing brood or in which there are residues of pollen.

The decrease in transparency following the thickening of the walls of cells can be traced back to the sedimentation of several types of organic matter associated with the rearing of larvae (honey, pollen or propolis) (Taha et al., 2010) or the metabolism of the larvae, such as, faeces, silken cocoon and pellicle (Free & Williams, 1974). The accumulation of organic matter results in a decrease in the volume and diameter of the brood cells (Karihaloo et al., 2013; Shawer et al., 2021).

There are other studies on the effect of the age of the comb on honey bee colonies (Al-Kahtani, 2018; Shawer et al., 2021). According to Berry & Delaplane (2001), colonies with new combs produce a greater area of brood, a greater area of sealed brood and the young bees are heavier. Interestingly, they report that brood survival in old combs is the only variable that is significantly higher. Taha & Al-Kahtani (2020) report a strong relationship between the thickness of residues in the comb and the activity of the honey bee colonies in collecting pollen, worker brood production, colony strength and honey yield. In comparison with colonies with 4-year-old combs, the number of returning workers, number of returning workers with pollen loads, rate of storing pollen, rate of worker brood production and size of the colony were significantly greater for those with younger combs. Eventually, old combs result in a lower honey yield of poor quality (Taha & El-Sanat, 2007; Taha et al., 2010).

The aim of the present study was to illustrate how modern imaging methods can be used for improving beekeeping, especially by revealing the inner structure of the comb using new tools like medical CT and  $\mu$ -CT. The necessity for regularly changing combs is unequivocally reinforced by our  $\mu$ -CT survey. The combined use of these two diagnostic techniques is unique and has great potential for improving beekeeping.

**ACKNOWLEDGMENTS.** We are indebted for the financial support from projects of the European Union, the European Social Fund: EFOP-3.6.3-VEKOP-16-2017-00008 and EFOP-3.6.3-VEKOP-16-2017-00005. The publication is supported by the János Bolyai Research Scholarship of the Hungarian Academy of Sciences (BO/00871/19). This research was done in collaboration with the Animal imaging core facility at the Szentágotthai Research Centre of the University of Pécs. We are grateful to Zs. Helyes for her help in the organizing this cooperation and for technical support.

**AUTHOR CONTRIBUTIONS.** T. Sipos and S. Keszthelyi designed the methodology and wrote the manuscript, T. Sipos and T. Donkó collected the research material and produced the samples, T. Donkó, T. Sipos and T. Kiss carried out the laboratory experiments; Á. Csóka, T. Donkó and S. Keszthelyi supported the research and evaluated the data. All authors read and approved the manuscript.

**CONFLICT OF INTEREST.** The authors declare that they have no conflict of interest.

## REFERENCES

- ALBA-ALEJANDRE I., ALBA-TERCEDOR J. & VEGA F.E. 2018: Micro-CT to document the coffee bean weevil, *Araecerus fasciculatus* (Coleoptera: Anthribidae), inside field-collected coffee berries (*Coffea canephora*). — *Insects* **9**: 100, 9 pp.
- AL-KAHTANI S.N. 2018: Morphometrical characteristics of Carniolan honeybee workers in relation to age of comb. — *Sci. J. King Faisal Univ. (Basic Appl. Sci.)* **19**: 47–54.
- BERRY J.A. & DELAPLANE K.S. 2001: Effects of comb age on honey bee colony growth and brood survivorship. — *J. Apic. Res.* **40**: 3–8.
- DAINAT B., VAN ENGELSDORP D. & NEUMANN P. 2012: Colony collapse disorder in Europe. — *Env. Microbiol. Rep.* **4**: 123–125.
- ELLIS R.A., WEIS T., SURYANARAYANAN S. & BEILIN K. 2020: From a free gift of nature to a precarious commodity: Bees, pollination services, and industrial agriculture. — *J. Agr. Chan.* **20**: 437–459.
- FACCHINI E., NALON L., ANDREIS M.E., DI GIANCAMILLO M., RIZZI R. & MORTARINO M. 2019: Honeybee pupal length assessed by CT-scan technique: effects of *Varroa* infestation, developmental stage and spatial position within the brood comb. — *Sci. Rep.* **9**: 10614, 6 pp.
- FEDOROV A., BEICHEL R., KALPATHY-CRAMER J., FINET J., FILLION-ROBIN J.C., PUJOL S., BAUER C., JENNINGS D., FENNESSY F.M., SONKA M., BUATTI J., AYLWARD S.R., MILLER J.V., PIEPER S. & KIKINIS R. 2012: 3D Slicer as an image computing platform for the quantitative imaging network. — *Magn. Reson. Imag.* **30**: 1323–1341.
- FREE J.B. & WILLIAMS I.H. 1974: Factors determining food storage and brood rearing in honey bee (*Apis mellifera* L.) comb. — *J. Entomol. (A)* **49**: 47–63.
- FRIEDRICH F., MATSUMURA Y., POHL H., BAI M., HÖRNSCHEMEYER T. & BEUTEL R.G. 2014: Insect morphology in the age of phylogenomics: innovative techniques and its future role in systematics. — *Entomol. Sci.* **17**: 1–24.
- GARIBALDI L.A., STEFFAN-DEWENTER I., WINFREE R., AIZEN M.A., BOMMARCO R., CUNNINGHAM S.A. & KLEIN A.M. 2013: Wild pollinators enhance fruit set of crops regardless of honey bee abundance. — *Science* **339**: 1608–1611.
- HEPBURN H.R. 1998: Reciprocal interactions between honey bees and combs in the integration of some colony functions in *Apis mellifera* L. — *Apidologie* **29**: 47–66.
- KARIHALOO B.L., ZHANG K. & WANG J. 2013: Honeybee combs: how the circular cells transform into rounded hexagons. — *J. R. Soc. Interf.* **10**: 20130299, 4 pp.
- KESZTHELYI S., PÖNYA Z., CSÓKA Á., BÁZÁR G., MORSCHHAUSER T. & DONKÓ T. 2020: Non-destructive imaging and spectroscopic techniques to investigate the hidden-lifestyle arthropod pests: a review. — *J. Plant Dis. Prot.* **127**: 283–295.
- KESZTHELYI S., SIPOS T., CSÓKA Á. & DONKÓ T. 2021: CT-supported analysis of the destructive effects of *Varroa destructor* on the pre-imaginal development of honey bee, *Apis mellifera*. — *Apidologie* **52**: 155–162.
- NEOV B., GEORGIEVA A., SHUMKOVA R., RADOSLAVOV G. & HRISTOV P. 2019: Biotic and abiotic factors associated with colonies mortalities of managed honey bee (*Apis mellifera*). — *Diversity* **11**: 237, 16 pp.
- SHAWER D.M., RAKHA O.M., TAHA E.K.A., AL-KAHTANI S.N. & ELNABAWY E.M. 2021: The impact of caging the queens during the flow season on some biological activities of honeybee colonies. — *Saudi J. Biol. Sci.* **28**: 2975–2979.
- SIPOS T., DONKÓ T., JÓCSÁK I. & KESZTHELYI S. 2021: Study of morphological features in pre-imaginal honey bee impaired by *Varroa destructor* by means of computer tomography. — *Insects* **12**: 717, 12 pp.
- SMITH D.B., BERNHARDT G., RAINE N.E., ABEL R.L., SYKES D., AHMED F., PEDROSO I. & GILL R.J. 2016: Exploring miniature insect brains using micro-CT scanning techniques. — *Sci. Rep.* **6**: 21768, 10 pp.
- SONENSHINE D.E., POSADA-FLOREZ F., LAUDIER D., GULBRONSON C.J., RAMSEY S. & COOK S.C. 2022: Histological atlas of the internal anatomy of female *Varroa destructor* (Mesostigmata: Varroidae) mites in relation to feeding and reproduction. — *Ann. Entomol. Soc. Am.* **115**: 163–193.
- TAHA E.K.A. & AL-KAHTANI S.N. 2020: The relationship between comb age and performance of honey bee (*Apis mellifera*) colonies. — *Saudi J. Biol. Sci.* **27**: 30–34.
- TAHA E.K.A. & EL-SANAT S.I. 2007: Effect of combs age on honey production and its physical and chemical properties. — *Bull. Entomol. Soc. Egypt* **2**: 9–18.
- TAHA E.K.A., MANOSUR H.M. & SHAWER M.B. 2010: The relationship between comb age and the amounts of mineral elements in honey and wax. — *Bee World* **49**: 202–207.
- WILLIAMS G.R., TARPY D.R., VAN ENGELSDORP D., CHAUZAT M.P., COX-FOSTER D.L., DELAPLANE K.S., NEUMANN P., PETTIS J.S., ROGERS R.E. & SHUTLER D. 2010: Colony Collapse Disorder in context. — *BioEssays* **32**: 845–846.
- WINFREE R., GROSS B.J. & KREMEN C. 2011: Valuing pollination services to agriculture. — *Ecol. Econ.* **71**: 80–88.
- WIPFLER B., POHL H., YAVORSKAYA M.I. & BEUTEL R.G. 2016: A review of methods for analysing insect structures – the role of morphology in the age of phylogenomics. — *Curr. Opin. Insect Sci.* **18**: 60–68.

Received July 18, 2022; revised and accepted November 21, 2022

Published online January 18, 2023